

Electronic Supplementary Information (ESI) for:

**Modulation of band gap and p- versus n-semiconductor character  
of ADA dyes by core and acceptor group variation**

*Agnieszka Nowak-Król,<sup>a</sup> Reinhard Wagener,<sup>a</sup> Felix Kraus,<sup>a</sup> Amaresh Mishra,<sup>b</sup> Peter Bäuerle,<sup>b</sup>  
and Frank Würthner\*<sup>a</sup>*

<sup>a</sup> Universität Würzburg, Institut für Organische Chemie & Center for Nanosystems Chemistry,  
Am Hubland, 97074 Würzburg, Germany.

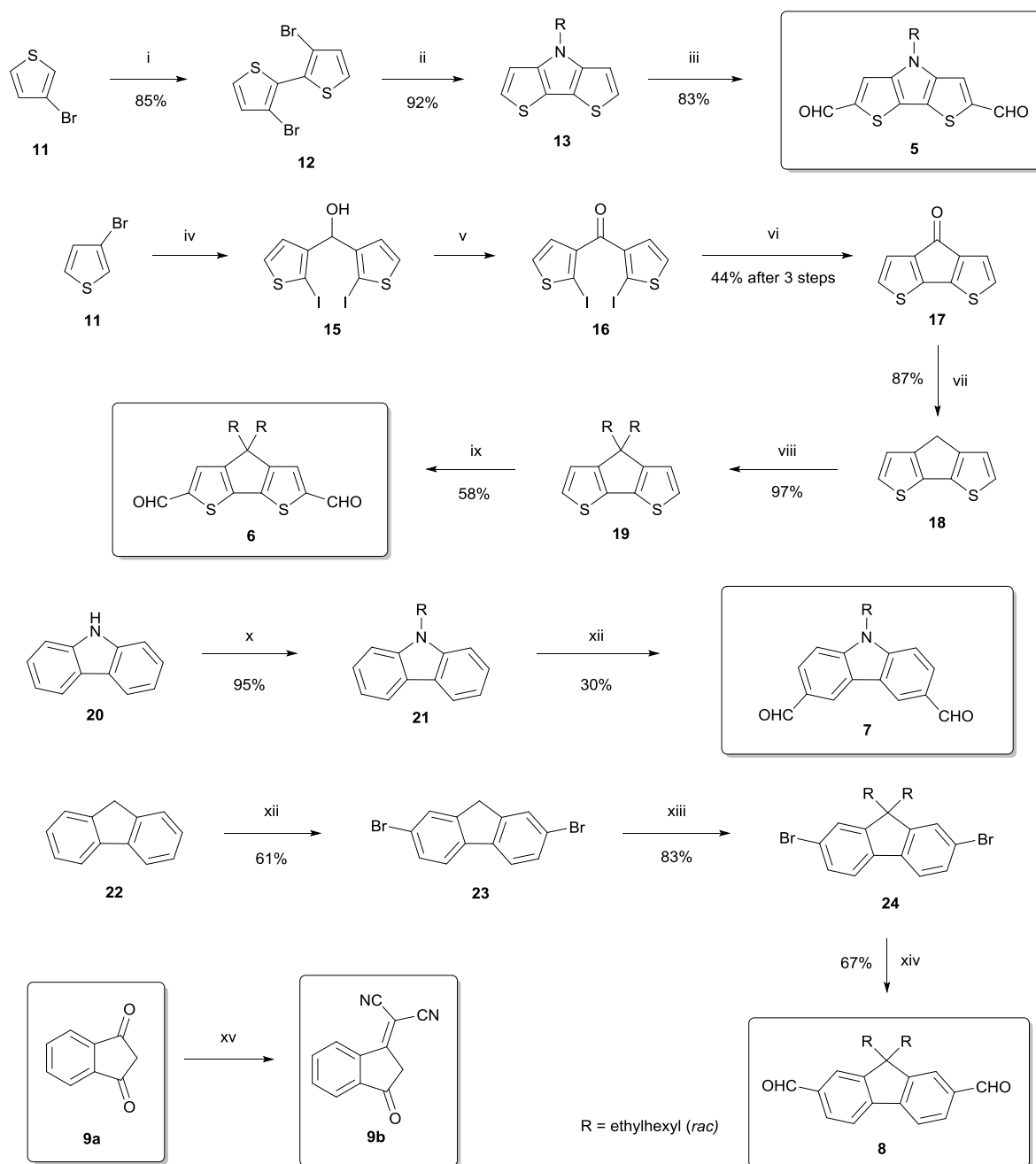
<sup>b</sup> Universität Ulm, Institute of Organic Chemistry II and Advanced Materials,  
Albert-Einstein-Allee 11, 89081 Ulm, Germany.

E-mail: wuerthner@chemie.uni-wuerzburg.de

## Table of Contents

|  |         |
|--|---------|
| <b>1. Synthesis</b> .....  | S1-S5   |
| <b>2. Absorption and photoluminescence</b> .....                   | S5-S7   |
| <b>3. Electrochemistry</b> .....                                   | S7      |
| <b>4. Calculation of HOMO, LUMO and band gaps</b> .....            | S8      |
| <b>5. DFT calculations</b> .....                                   | S8-S9   |
| <b>6. Differential scanning calorimetry</b> .....                  | S10-S11 |
| <b>7. Organic thin film transistors and AFM measurements</b> ..... | S11-S12 |
| <b>8. References</b> .....   | S12-S13 |
| <b>9. NMR spectra</b> .....  | S14-S24 |
| <b>10. MS spectra</b> .....  | S25     |

## 1. Synthesis of building blocks



**Scheme 1** Synthesis of building blocks **5**, **6**, **7**, **8**, and **9b**. i) 1. LDA, 0 °C, 3.5 h; 2. ZnCl<sub>2</sub>, 0 °C, 45 min; 3. CuCl<sub>2</sub>, -78 °C to RT, 18 h. ii) RNH<sub>2</sub> (*rac*), Pd<sub>2</sub>(dba)<sub>3</sub>, BINAP, NaO<sup>t</sup>Bu, toluene, 110 °C, 25 h. iii) 1. POCl<sub>3</sub>, DMF, 130 °C, 12 h; 2. 1 M NaOH (aq.), DCM, RT, 2 h. iv) 1. <sup>n</sup>BuLi, Et<sub>2</sub>O, -78 °C, 1 h, then RT, 1 h. 2. 3-thiophenecarboxaldehyde (**14**), -78 °C, 30 min, then RT, 3 h; 3. <sup>n</sup>BuLi, -78 °C, 40 min, then RT, 2 h; 4. I<sub>2</sub>, Et<sub>2</sub>O, -20 °C, RT, 13.5 h. v) PCC, DCM, RT, 22 h. vi) Cu, DMF, 120 °C, 4 h. vii) 1. hydrazine hydrate, OHCH<sub>2</sub>CH<sub>2</sub>OH, 100 °C, 1 h; 2. KOH, H<sub>2</sub>O, 180 °C, 3 h. viii) 1. 1.05 eq. <sup>n</sup>BuLi, THF, -78 °C, 1 h, then RT, 1 h; 2. 1.05 eq. RBr (*rac*), -78 °C, 30 min, then RT, 2 h; 3. 1.05 eq. <sup>n</sup>BuLi, THF, -78 °C, 1 h, then RT, 1 h; 4. 1.05 eq. RBr (*rac*), -78 °C, 30 min, then RT, 2 h. ix) DMF, POCl<sub>3</sub>, DCE, 90 °C, 2 d. x) RBr (*rac*), NaOH (aq.), TBAB, toluene, reflux, 16 h. xi) DMF, POCl<sub>3</sub>, 100 °C, 16 h. xii) Br<sub>2</sub>, CHCl<sub>3</sub>, RT, 20 h. xiii) RBr (*rac*), NaO<sup>t</sup>Bu, THF, RT, 16 h. xiv) 1. <sup>n</sup>BuLi, THF, -78 °C, 40 min; DMF, -78 °C, 1 h, then RT, 1 h. xv) malononitrile, NaOAc, EtOH, RT, 40 min.

The starting material for the preparation of both bithiophene-containing donor cores was 3-bromothiophene (**11**). The synthesis of dialdehyde **5** encompassed three steps.<sup>S1-S3</sup> Initial oxidative aromatic coupling of **11** provided bithiophene **12**,<sup>S1</sup> which was submitted to Buchwald-Hartwig amination.<sup>S2</sup> The reaction employing Pd<sub>2</sub>dba<sub>3</sub>, 2,2'-bis(diphenylphosphino)-1,1'-binaphthyl (BINAP), and NaO<sup>t</sup>Bu produced DTP **13** in 92%. The sequence of the reactions was closed by Vilsmeier-Haack formylation.<sup>S3</sup>

Building block **6** was readily obtained in a six-step synthesis. Bis(2-iodo-3-thienyl)methanol (**15**) was prepared according to the reported procedure<sup>S4</sup> in one pot from bromide **11** by its lithiation, followed by the reaction with 3-thiophenecarboxaldehyde (**14**), subsequent dilithiation and final reaction with iodine. Further, crude product was oxidized by PCC to ketone **16**, which was finally converted into **17** *via* intramolecular Ullman reaction in 44% overall yield of the three synthetic steps.<sup>S4</sup> In the next, step **17** was reduced *via* Wolff-Kishner reaction to afford **18** in 87% yield.<sup>S4</sup> Consecutive alkylation thereof gave **19** in 97%. The synthesis was accomplished by Vilsmeier-Haack formylation that produced donor core CPDT **6** in 58% yield.<sup>S5</sup>

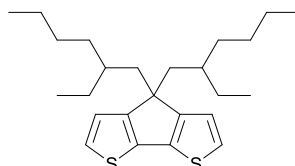
The preparation of carbazole building block was straightforward. To obtain **21** from carbazole (**20**), we applied a phase-transfer catalysis (PTC) methodology using ethylhexyl bromide as an alkylating agent and tetrabutylammonium bromide (TBAB) as a PTC catalyst.<sup>S6</sup> The following Vilsmeier-Haack formylation afforded compound **7** in a moderate yield. Likewise, compound **8** could be easily prepared starting from commercially available fluorene (**22**). Bromination<sup>S7</sup> followed by alkylation<sup>S8</sup> afforded compound **24**, which was subsequently transformed into dialdehyde **8** by applying <sup>t</sup>BuLi and DMF. Acceptor **9b** was prepared following the procedure by Robertson.<sup>S9</sup>

## General

All reagents were purchased from commercial sources and used as received without further purification, unless otherwise stated. Reagent grade solvents were distilled prior to use. Column chromatography was performed on silica (silica gel, 230-400 mesh). <sup>1</sup>H NMR spectra were recorded on a Bruker Avance 400 spectrometer at room temperature, unless otherwise noted, and calibrated to the residual solvent signals or TMS. *J* values are given in Hz. Carbazole (**20**), 2-ethylhexyl bromide, fluorene (**22**), 3-bromothiophene (**11**), 3-thiophenecarboxaldehyde (**14**), and 1,3-indandione (**9a**) were commercially available.

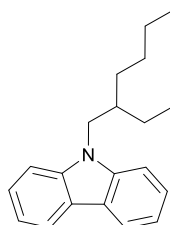
Compounds **12**,<sup>S1</sup> **13**,<sup>S2</sup> **5**,<sup>S3</sup> **15**,<sup>S4</sup> **16**,<sup>S4</sup> **17**,<sup>S4</sup> **18**,<sup>S4</sup> **6**,<sup>S5</sup> **23**,<sup>S7</sup> **24**,<sup>S8</sup> and **9b**<sup>S9</sup> were prepared according to the literature procedures.

### Synthesis of compound **19**.



Compound **19** was synthesized by adopting the reported procedure.<sup>S4</sup> A solution of compound **18** (1.65 g, 9.26 mmol) in THF (50 mL) was cooled to  $-78$  °C under nitrogen. Then the following operations were conducted: a) <sup>n</sup>BuLi (2.5 M in hexane; 3.9 mL, 9.72 mmol) was added dropwise and the mixture was kept at  $-78$  °C for 1 h, followed by 1 h at room temperature; b) the mixture was again cooled to  $-78$  °C, 2-ethylhexyl bromide (1.74 mL, 9.72 mmol) was added and after 30 min the reaction was stirred at room temperature for 2 h. Next, steps a) and b) were repeated using the same amounts of reagents. Afterwards, the solution was extracted with diethyl ether, washed with water, brine, NH<sub>4</sub>Cl (aq.) and dried over MgSO<sub>4</sub>. The crude product was purified by column chromatography (silica, pentane) to obtain **19** (3.62 g, 97%) as a light yellow oil. Compound **19** was obtained as a mixture of stereoisomers. <sup>1</sup>H NMR (400 MHz, CD<sub>2</sub>Cl<sub>2</sub>)  $\delta$  7.14 (d,  $J = 4.9$  Hz, 2H), 6.99-6.94 (m, 2H), 2.00-1.75 (m, 4H), 1.44-1.17 (m, 2H), 1.07-0.83 (m, 16H), 0.83-0.69 (m, 6H), 0.64-0.54 (m, 8H). Analytical data are in accordance with the literature.<sup>S10</sup>

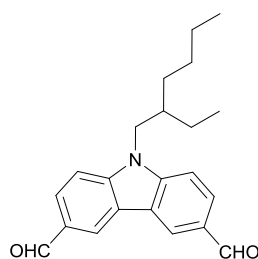
### Synthesis of compound **21**.



Compound **21** was synthesized by adopting the reported procedure.<sup>S11</sup> To a solution of carbazole (**20**, 1.197 g, 7.16 mmol) and tetrabutylammonium bromide (46 mg, 0.14 mmol) in toluene (12 mL) NaOH (50% w/w; 4.6 g, 57.3 mmol) was added. Next, 2-ethylhexyl bromide

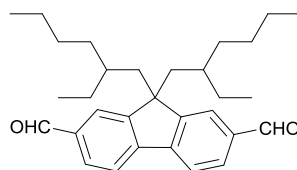
(1.60 g, 8.30 mmol) was added dropwise at RT to the mixture and the reaction was continued for 16 h under reflux. Afterwards, the layers were separated. The organic solvent was evaporated *in vacuo* and the residue was dissolved in CH<sub>2</sub>Cl<sub>2</sub>, washed with water and dried over MgSO<sub>4</sub>. After filtration solvent was removed under reduced pressure and the crude product was purified by Kugelrohr distillation to afford **21** (1.90 g, 95%) as a yellowish oil. <sup>1</sup>H NMR (400 MHz, CDCl<sub>3</sub>) δ 8.14-8.07 (m, 2H), 7.50-7.36 (m, 4H), 7.25-7.19 (m, 2H), 4.26-4.07 (m, 2H), 2.15-1.99 (m, 1H), 1.47-1.18 (m, 8H), 0.92 (t, *J* = 7.4 Hz, 3H), 0.87 (t, *J* = 7.2 Hz, 3H). Analytical data are in accordance with the literature.<sup>S12</sup>

### Synthesis of compound 7.



Compound **7** was prepared by adopting the reported procedure.<sup>S13</sup> A Schlenk tube was charged with dimethylformamide (24.20 g, 331 mmol) and the solvent was cooled to 0 °C. Then phosphorus oxichloride (50.76 g, 331 mmol) was added dropwise and the solution was stirred at 0 °C for 1 h. Next, compound **21** (5.00 g, 17.89 mmol) was added and the reaction mixture was stirred at 100 °C for 16 h. After cooling to 0 °C, the mixture was neutralized by adding NaOH solution (1 M). The product was extracted with CH<sub>2</sub>Cl<sub>2</sub>, washed with water and dried over Na<sub>2</sub>SO<sub>4</sub>. Column chromatography (silica, EtOAc/hexane 1:9 to 2:9) afforded **7** (1.82 g, 30 %) as a colorless solid. <sup>1</sup>H NMR (400 MHz, CDCl<sub>3</sub>) δ 10.14 (s, 2H), 8.67 (dd, *J* = 1.6, 0.5 Hz, 2H), 8.08 (dd, *J* = 8.6, 1.6 Hz, 2H), 7.54 (d, *J* = 8.6 Hz, 2H), 4.26 (d, *J* = 7.6 Hz, 2H), 2.14-2.00 (m, 1H), 1.49-1.20 (m, 8H), 0.94 (t, *J* = 7.4 Hz, 3H), 0.85 (t, *J* = 7.1 Hz, 3H). Analytical data are in accordance with the literature.<sup>S3</sup>

## Synthesis of compound **8**.



A dried flask was charged with dibromofluorene **23** (104 mg, 0.19 mmol). The vessel was purged with nitrogen and closed with a septum. Afterwards, anhydrous THF (0.79 mL) was added and the solution was cooled under nitrogen to  $-78\text{ }^{\circ}\text{C}$ . Next, BuLi (2.5 M in hexane; 0.23 mL, 0.58 mmol,) was added dropwise over 5 min and the mixture was stirred at  $-78\text{ }^{\circ}\text{C}$  for ca. 40 min, followed by addition of anhydrous DMF (50  $\mu\text{L}$ , 0.65 mmol) in THF (85  $\mu\text{L}$ ). The reaction was stirred at this temperature for 1 h. Then, the cooling bath was removed and the stirring was continued for 1 h. Afterwards, the reaction was quenched with a saturated aqueous  $\text{NH}_4\text{Cl}$ , and extracted with  $\text{Et}_2\text{O}$ . The combined organic extracts were dried over anhydrous  $\text{Na}_2\text{SO}_4$ , filtered, and evaporated. A crude product was purified by column chromatography (silica, hexane/EtOAc 19:1) to give **8** (57 mg, 67%) as a colorless solid. Compound **8** was obtained as a mixture of stereoisomers.  $^1\text{H}$  NMR (400 MHz,  $\text{CDCl}_3$ )  $\delta$  10.09 (s, 2H), 7.99-7.95 (m, 2H), 7.95-7.89 (m, 4H), 2.14-2.03 (m, 4H), 0.94-0.70 (m, 12H), 0.70-0.57 (m, 10H), 0.52-0.44 (m, 6H), 0.44-0.35 (m, 2H). Analytical data are in accordance with the literature.<sup>S14</sup>

## 2. Absorption and photoluminescence

UV/vis measurements were performed using Lambda 950 or Lambda 35 (Perkin-Elmer). All spectra were measured in dichloromethane (spectrophotometric grade) from Merck (Hohenbrunn, Germany) at a concentration of about  $10^{-5}\text{ M}^{-1}$ . Fluorescence spectra were recorded on a QM-4/2003 (PTI) using the optical dilution method ( $\text{OD} < 0.05$ ).<sup>S15</sup> Absolute fluorescence quantum yields were measured on the Hamamatsu instrument equipped with an integrating sphere. The photoluminescence quantum yields of 4% and 2% were determined for compounds **1a** and **2a**, respectively. For other compounds the emission was below 1% and could not be quantified with our instrument.

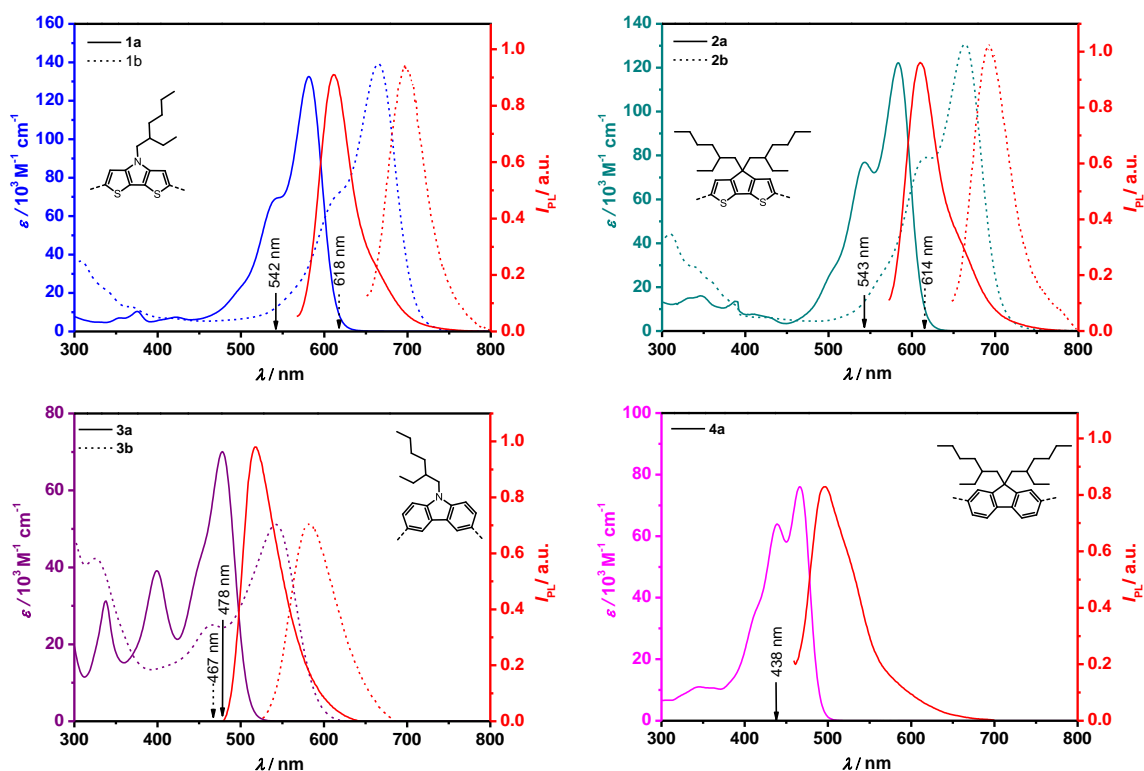


**Fig. S1** Absorption (blue, cyan, purple, pink lines) and corresponding photoluminescence spectra (red lines) of dyes **1a**, **1b**, **2a**, **2b**, **3a**, **3b**, and **4a** (UV/vis:  $\text{CH}_2\text{Cl}_2$ ,  $\sim 10^{-5}$  M, 298 K; Photoluminescence:  $\text{CH}_2\text{Cl}_2$ ,  $\sim 10^{-7}$  M, 298 K). Solid lines present the spectra of compounds with IND acceptors, whereas dotted lines correspond to the spectra of DCIND derivatives.

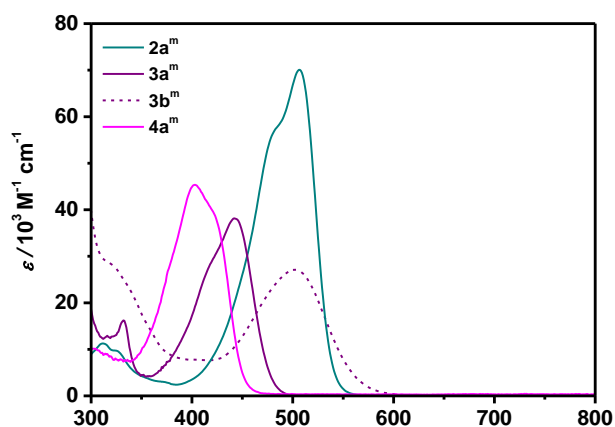


**Fig. S2** UV/vis spectra of mono-substituted dyes **2a<sup>m</sup>**, **3a<sup>m</sup>**, **3b<sup>m</sup>** and **4a<sup>m</sup>** ( $\text{CH}_2\text{Cl}_2$ ,  $\sim 10^{-5}$  M, 298 K). Solid lines present the spectra of compounds with IND acceptors, whereas a dotted line corresponds to the spectrum of a DCIND derivative.

**Table S1** Optical properties of the mono-substituted dyes in CH<sub>2</sub>Cl<sub>2</sub> ( $c = 2 \cdot 10^{-5}$  M).

| Dye                   | $\lambda_{\text{abs}}^a$ [nm] | $\epsilon_{\text{max}}^b$ [ $10^3 \text{ M}^{-1} \text{ cm}^{-1}$ ] | $\mu_{\text{eg}}^2$ [ $\text{D}^2$ ] |
|-----------------------|-------------------------------|---|--------------------------------------|
| <b>2a<sup>m</sup></b> | 507                           | 70.1  | 93                                   |
| <b>3a<sup>m</sup></b> | 442                           | 37.9  | 53                                   |
| <b>3b<sup>m</sup></b> | 502                           | 27.1  | 49                                   |
| <b>4a<sup>m</sup></b> | 403                           | 45.4  | 70                                   |

<sup>a</sup> Absorption maximum. <sup>b</sup> Molar absorption coefficient. <sup>c</sup> Square transition dipole moments calculated from the measured data.

### 3. Electrochemistry

Details regarding the CV measurements are given in the main text.

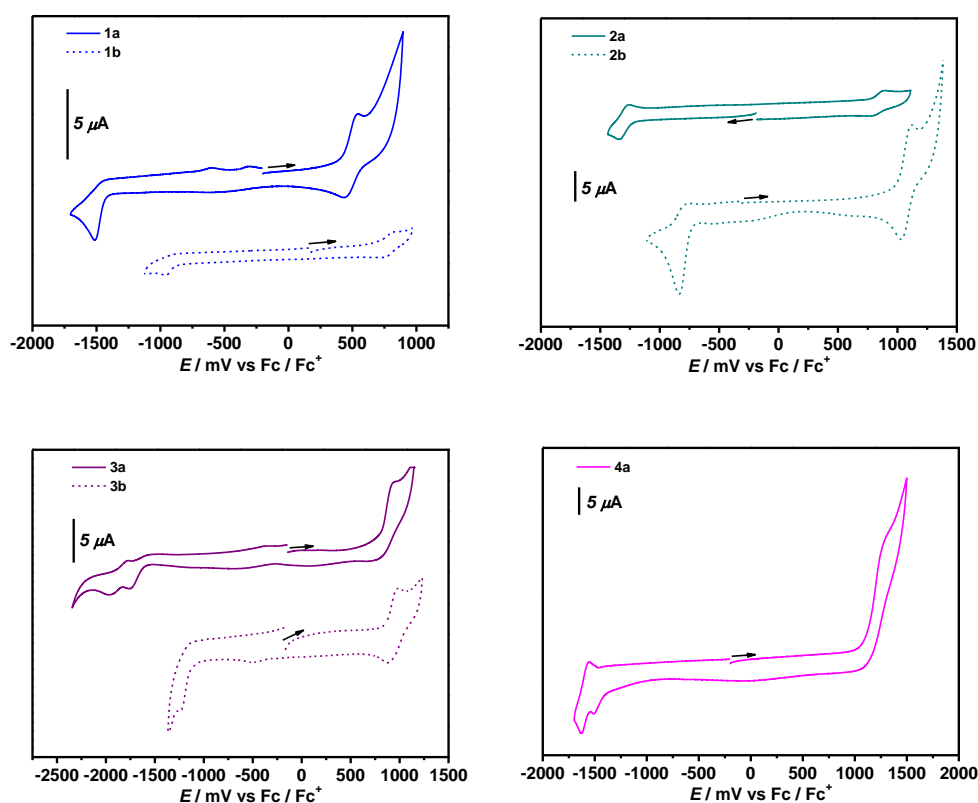


**Fig. S3** Cyclic voltammograms of **1a**, **1b**, **2a**, **2b**, **3a**, **3b**, and **4a** (CH<sub>2</sub>Cl<sub>2</sub>,  $\sim 10^{-4} - 10^{-5}$  M, 298 K; scan rate:  $100 \text{ mV s}^{-1}$ ; supporting electrolyte: Bu<sub>4</sub>NPF<sub>6</sub> (0.1 M); calibrated vs. Fc/Fc<sup>+</sup> as an internal standard). Solid lines present voltammograms of compounds with IND acceptors, whereas dotted lines correspond to the voltammograms of DCIND derivatives.

#### 4. Calculation of HOMO, LUMO and band gaps

The HOMO/LUMO energy levels were calculated according to the following equations:

$$E_{\text{HOMO}} = -e E_{1/2}^{\text{ox}} - 5.15 \text{ eV.}$$

$$E_{\text{LUMO}} = E_{\text{HOMO}} + (hc/\lambda_{\text{max}}).$$

The optical band gaps were calculated using the equation:  $E_{\text{gap}} = E_{\text{HOMO}} - E_{\text{LUMO}} = hc/\lambda_{\text{max}}$ .

The electrochemical band gaps were calculated with  $E_{\text{g}}^{\text{CV}} = E_{1/2}^{\text{ox}} - E_{1/2}^{\text{red}}$ . The deviation between electrochemical and the optical band gap is at about  $\pm 0.1$  eV.

**Table S2** Optical and electrochemical properties of investigated ADA systems.

| Dye       | $E_{1/2}^{\text{red}^a}$<br>[V] | $E_{1/2}^{\text{ox}^a}$<br>[V] | $\lambda_{\text{max}}^b$<br>[nm] | $E_{\text{HOMO}}^c$<br>[eV] | $E_{\text{LUMO}}^d$<br>[eV] | $E_{\text{g}}^{\text{opt}^e}$<br>[eV] | $E_{\text{g}}^{\text{CV}^f}$<br>[eV] |
|-----------|---------------------------------|--------------------------------|----------------------------------|-----------------------------|-----------------------------|---------------------------------------|--------------------------------------|
| <b>1a</b> | -1.52 <sup>g</sup>              | +0.49                          | 582                              | -5.64                       | -3.51                       | 2.13                                  | 2.01                                 |
| <b>1b</b> | -0.96 <sup>g</sup>              | +0.83 <sup>g</sup>             | 665                              | -5.98                       | -4.12                       | 1.86                                  | 1.79                                 |
| <b>2a</b> | -1.30                           | +0.84                          | 584                              | -5.99                       | -3.87                       | 2.12                                  | 2.14                                 |
| <b>2b</b> | -0.84 <sup>g</sup>              | +1.08                          | 664                              | -6.23                       | -4.36                       | 1.87                                  | 1.92                                 |
| <b>3a</b> | -1.76 <sup>g</sup>              | +0.97 <sup>g</sup>             | 478                              | -6.12                       | -3.53                       | 2.59                                  | 2.73                                 |
| <b>3b</b> | -1.25 <sup>g</sup>              | +0.93                          | 542                              | -6.08                       | -3.79                       | 2.29                                  | 2.18                                 |
| <b>4a</b> | -1.51 <sup>g</sup>              | +1.26 <sup>g</sup>             | 466                              | -6.41                       | -3.75                       | 2.66                                  | 2.77                                 |

<sup>a</sup> Redox potentials vs. Fc/Fc<sup>+</sup> in CH<sub>2</sub>Cl<sub>2</sub> ( $c \sim 10^{-4} - 10^{-5}$  M); scan rate: 100 mV s<sup>-1</sup>; supporting electrolyte: Bu<sub>4</sub>NPF<sub>6</sub> (0.1 M). <sup>b</sup> Absorption maximum. <sup>c</sup>  $E_{\text{HOMO}} = -e E_{1/2}^{\text{ox}} - 5.15$  eV. <sup>d</sup>  $E_{\text{LUMO}} = E_{\text{HOMO}} + (hc/\lambda_{\text{max}})$ . <sup>e</sup>  $E_{\text{g}}^{\text{opt}} = E_{\text{HOMO}} - E_{\text{LUMO}}$ . <sup>f</sup>  $E_{\text{g}}^{\text{CV}} = E_{1/2}^{\text{ox}} - E_{1/2}^{\text{red}}$ . <sup>g</sup> Peak potential.

#### 5. DFT calculations

DFT calculations were performed for a simplified model compound of **1a**, **1b**, **2a**, **2b**, **3a**, **3b**, **4a**, and **4b** (ethylhexyl chains were replaced by methyl groups) by using the Gaussian 09 program package<sup>S16</sup> with B3-LYP<sup>S17</sup> as a functional and def2-SVP<sup>S18</sup> as a basis set. The structures were geometry optimized, followed by frequency calculations on the optimized structures which confirmed the existence of a minimum.

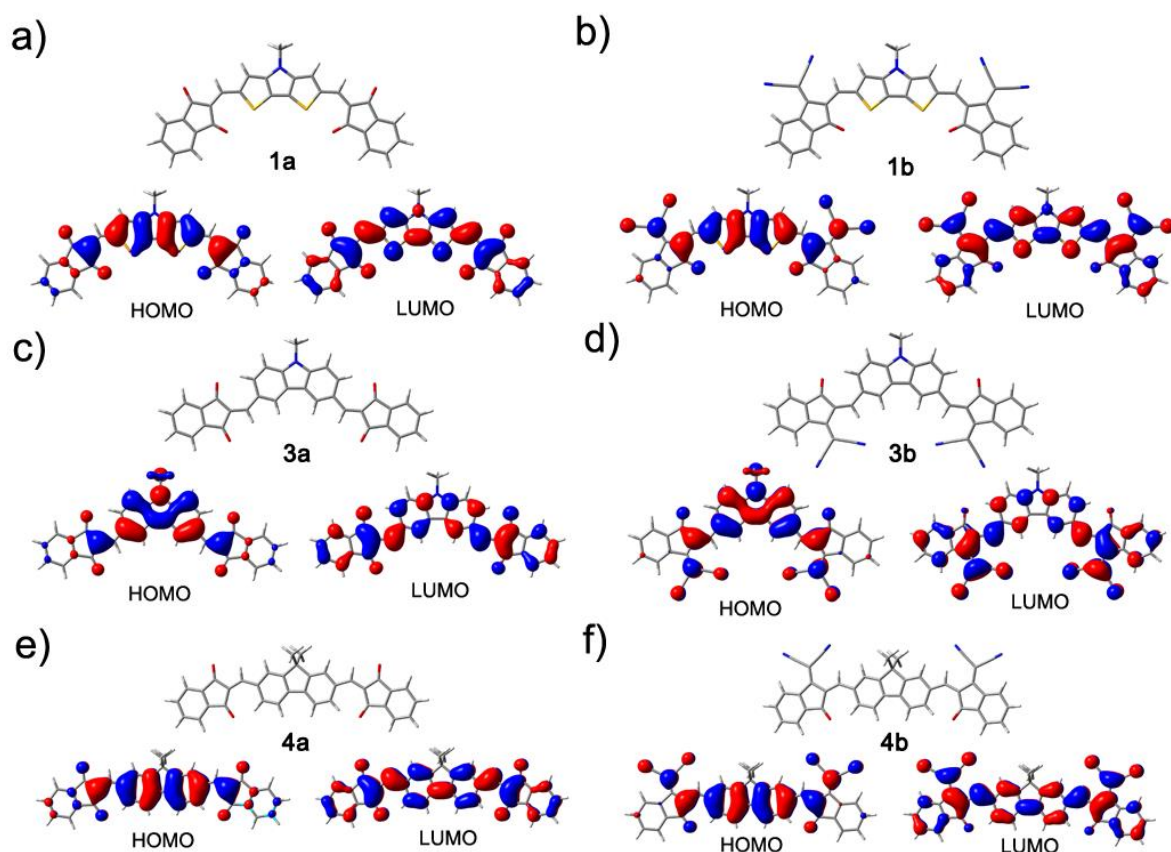


**Fig. S4** Geometry optimized structures (with B3LYP/def2-SVP) as well as orbital contour plots of HOMO and LUMO for model compounds of a) **1a**, b) **1b**, c) **3a**, d) **3b**, e) **4a**, and f) **4b** (ethylhexyl substituents replaced with methyl groups).

**Table S3** Calculated HOMO/LUMO levels and energy gaps ( $E_g$ ).

| Dye                    | $E_{\text{HOMO}}$ [eV] | $E_{\text{LUMO}}$ [eV] | $E_g$ [eV] |
|------------------------|------------------------|------------------------|------------|
| <b>1a</b>              | -5.75                  | -3.21                  | 2.54       |
| <b>1b</b>              | -6.07                  | -3.84                  | 2.23       |
| <b>2a</b>              | -5.79                  | -3.29                  | 2.50       |
| <b>2b</b>              | -6.10                  | -3.89                  | 2.21       |
| <b>3a</b>              | -6.02                  | -2.78                  | 3.24       |
| <b>3b</b>              | -6.25                  | -3.39                  | 2.86       |
| <b>4a</b>              | -6.19                  | -3.15                  | 3.04       |
| <b>4b</b> <sup>a</sup> | -6.44                  | -3.74                  | 2.70       |

<sup>a</sup> Compound could not be isolated.

## 6. Differential scanning calorimetry

Differential scanning calorimetry (DSC) measurements were carried out under nitrogen atmosphere using DSC Q1000 (TA Instruments) at a heating rate/cooling rate of 10 K min<sup>-1</sup>. At least two heating-cooling cycles were measured.

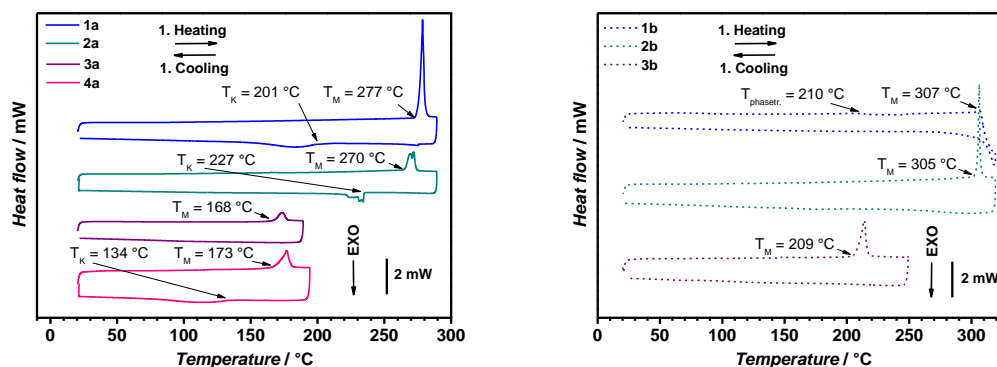


**Fig. S5** DSC curves (heating and cooling) for molecules with IN acceptors (left) and with DCNIO acceptors (right) (heating rate/cooling rate 10 K min<sup>-1</sup>, N<sub>2</sub>).

Fig. S5 displays first cycles (heating and first cooling) of DSC measurements. Thermograms of **1a**, **2b** and **4a** show weak exothermic peaks on cooling which correspond to isotropic to glassy state transitions, whereas molecule **1b** decomposes upon melting. Calorimetric data are listed in Table S4.

**Table S4** Calorimetric data for ADA dyes.

| Dye       | $T_M$ [°C] <sup>a</sup> | $T_p$ [°C] <sup>b</sup> | $\Delta H$ [kJ mol <sup>-1</sup> ] <sup>c</sup> |
|-----------|-------------------------|-------------------------|---|
| <b>1a</b> | 277                     | 278.64                  | 58.1  |
| <b>1b</b> | 307 <sup>d</sup>        | —                       | —   |
| <b>2a</b> | 270                     | 272.04                  | 11.4  |
| <b>2b</b> | 305                     | 306.22                  | 46.9  |
| <b>3a</b> | 168                     | 174.00                  | 16.6  |
| <b>3b</b> | 209                     | 213.82                  | 44.0  |
| <b>4a</b> | 173                     | 176.69                  | 23.8  |

<sup>a</sup> Melting point determined from the peak onset temperature. <sup>b</sup> Peak temperature. <sup>c</sup> Enthalpy change. <sup>d</sup> Decomposition upon melting.

To calculate thermodynamic data for **2a** curve-fitting of the melting peak had to be performed.

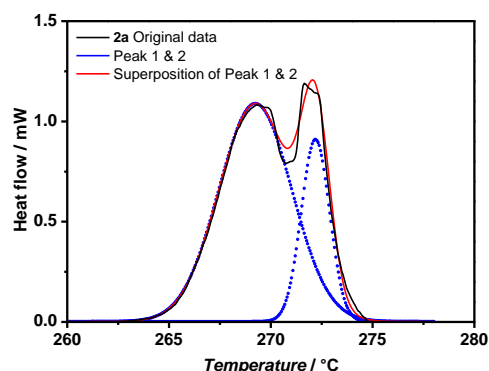


**Fig. S6** The first and second phase transitions of **2a** fitted with two gaussians.

## 7. Organic thin film transistors and AFM measurements

### 1.1. Substrates for organic thin film transistor fabrication

Silicon wafers were used as gate electrodes, consisting of boron doped n-type silicon and a 100 nm layer of SiO<sub>2</sub> (gate dielectric;  $C_i = 34 \text{ nF cm}^{-2}$ ). These wafers were modified with a thin layer of AlO<sub>x</sub> (8 nm) and a monolayer of *n*-tetradecylphosphonic acid (TPA; 1.7 nm;  $C_i = 32.4 \text{ nF cm}^{-2}$ ).<sup>S19</sup> The wafers were cleaned by spin coating with toluene, acetone and isopropanol (3000 rpm s<sup>-1</sup>, 30 s), before device preparation.

### 1.2. Sublimation of organic material and preparation of top contacts

Thin layers of the molecules (30 nm) were sublimed using the AUTO306/FL400 (Boc Edwards) or the EVAP300 (Creaphys). Sublimation took place at about  $2 \cdot 10^{-6}$  mbar. The sublimation rate was in the range of 0.2-0.6 nm min<sup>-1</sup>. Sublimation and substrate temperature were different for each molecule and for compounds **2a** and **2b** are given in Table S5.

**Table S5** Sublimation temperature,<sup>a</sup> substrate temperature,<sup>b</sup> and the instrument used for processing.<sup>c</sup>

| Dye       | $T_{\text{SUB}} [^{\circ}\text{C}]^a$ | $T_{\text{substrate}} [^{\circ}\text{C}]^b$ | Instrument <sup>c</sup> |
|-----------|---------------------------------------|---|-------------------------|
| <b>2a</b> | 160                                   | 130   | EVAP300                 |
| <b>2b</b> | 195                                   | 150   | EVAP300                 |

Top electrodes were prepared using the same instruments by subliming a 30 nm layer of gold on top of the organic thin film. Shadow masks with square recesses (200  $\mu\text{m}$  x 200  $\mu\text{m}$ ) were used providing devices with a length  $L$  and width  $W$  of 100  $\mu\text{m}$  and 200  $\mu\text{m}$ , respectively. The deposition rate was in the range of 0.2-0.6  $\text{\AA s}^{-1}$ .

### 1.3 Atomic force microscopy

Atomic force microscopy (AFM) images were measured with a Multimode 8 AFM (Bruker), operating in tapping mode in air. Cantilevers OMCL-AC160-TS (Olympus) were used (resonance frequency  $\sim$  300 kHz; spring constant  $\sim$  40  $\text{Nm}^{-1}$ ).

## 8. References

- <sup>S1</sup> a) S. C. Rasmussen and S. J. Evenson, *Prog. Polym. Sci.* 2013, **38**, 1773; b) S. J. Evenson and S. C. Rasmusen, *Org. Lett.*, 2010, **12**, 4054.
- <sup>S2</sup> X. Hu, M. Shi, L. Zuo, Y. Nan, Y. Liu, L. Fu and H. Chen, *Polymer*, 2011, **52**, 2559.
- <sup>S3</sup> A. Yassin, T. Rousseau, P. Leriche, A. Cravino and J. Roncali, *Sol. Ener. Mater. Sol. Cells*, 2011, **95**, 462.
- <sup>S4</sup> C.-Y. Yu and C.-Y. Wu, *Dyes Pigm.*, 2014, **106**, 81.
- <sup>S5</sup> H. Padhy, D. Sahu, D. Patra, M. K. Pola, J.-H. Huang, C.-W. Chu, K.-H. Wei and H.-C. Lin, *J. Polym. Sci. A Polym. Chem.*, 2011, **49**, 3417.
- <sup>S6</sup> H.-Y. Wang, J.-J. Shi, G. Chen, X.-P. Xu and S.-J. Ji, *Synth. Met.*, 2012, **162**, 241.
- <sup>S7</sup> Q. Li, H. Guo, L. Ma, W. Wu, Y. Liu and J. Zhao, *J. Mater. Chem.* 2012, **22**, 5319.
- <sup>S8</sup> K. N. Winzenberg, P. Kemppinen, F. H. Scholes, G. E. Collis, Y. Shu, T. Birendra Singh, A. Bilic, C. M. Forsyth and S. E. Watkins, *Chem. Commun.*, 2013, **49**, 6307.
- <sup>S9</sup> M. Planells and N. Robertson, *Eur. J. Org. Chem.*, **2012**, 4947.
- <sup>S10</sup> C.-H. Chen, C.-H. Hsieh, M. Dubosc, Y.-J. Cheng and C.-S. Hsu, *Macromolecules*, 2010, **43**, 697.
- <sup>S11</sup> J.-H. Lee, J.-W. Park and S.-K. Choi, *Synth. Met.*, 1997, **88**, 31.
- <sup>S12</sup> H. Meng, Z.-K. Chen, X.-L. Liu, Y.-H. Lai, S.-J. Chua and W. Huang, *Phys. Chem. Chem. Phys.*, 1999, **1**, 3123.
- <sup>S13</sup> Y. Song, C. Di, Z. Wei, T. Zhao, W. Xu, Y. Liu, D. Zhang and D. Zhu, *Chem. Eur. J.*, 2008, **14**, 4731.

- <sup>S14</sup> P. Auragudom, A. A. Tangonan, M. A. G. Namboothiry, D. L. Carroll, R. C. Advincula, S. Phanichphant and T. R. Lee, *J. Polym. Res.*, 2010, **17**, 347.
- <sup>S15</sup> J. R. Lakowicz, *Principles of Fluorescence Spectroscopy*, Kluwer Academic/Plenum Publishers, New York, 1999.
- <sup>S16</sup> Gaussian 09, Revision D.01, M. J. Frisch, G. W. Trucks, H. B. Schlegel, G. E. Scuseria, M. A. Robb, J. R. Cheeseman, G. Scalmani, V. Barone, B. Mennucci, G. A. Petersson, H. Nakatsuji, M. Caricato, X. Li, H. P. Hratchian, A. F. Izmaylov, J. Bloino, G. Zheng, J. L. Sonnenberg, M. Hada, M. Ehara, K. Toyota, R. Fukuda, J. Hasegawa, M. Ishida, T. Nakajima, Y. Honda, O. Kitao, H. Nakai, T. Vreven, J. A. Jr. Montgomery, J. E. Peralta, F. Ogliaro, M. Bearpark, J. J. Heyd, E. Brothers, K. N. Kudin, V. N. Staroverov, T. Keith, R. Kobayashi, J. Normand, K. Raghavachari, A. Rendell, J. C. Burant, S. S. Iyengar, J. Tomasi, M. Cossi, N. Rega, J. M. Millam, M. Klene, J. E. Knox, J. B. Cross, V. Bakken, C. Adamo, J. Jaramillo, R. Gomperts, R. E. Stratmann, O. Yazyev, A. J. Austin, R. Cammi, C. Pomelli, J. W. Ochterski, R. L. Martin, K. Morokuma, V. G. Zakrzewski, G. A. Voth, P. Salvador, J. J. Dannenberg, S. Dapprich, A. D. Daniels, O. Farkas, J. B. Foresman, J. V. Ortiz, J. Cioslowski and D. J. Fox, Gaussian, Inc., Wallingford CT, 2013.
- <sup>S17</sup> (a) A. D. Becke, *Phys. Rev. A*, 1988, **38**, 3098; (b) C. Lee and W. Yang and R. G. Parr, *Phys. Rev. B*, 1988, **37**, 785; (c) A. D. Becke, *J. Chem. Phys.*, 1993, **98**, 5648.
- <sup>S18</sup> F. Weigand and R. Ahlrichs, *Phys. Chem. Chem. Phys.*, 2005, **7**, 3297–3305.
- <sup>S19</sup> (a) U. Kraft, M. Sejfić, M. J. Kang, K. Takimiya, T. Zaki, F. Letzkus, J. N. Burghartz, E. Weber and H. Klauk, *Adv. Mater.*, 2015, **27**, 207; (b) A. Liess, M. Stolte, T. He and F. Würthner, *Mater. Horiz.*, 2016, **3**, 72.

## 9. NMR spectra

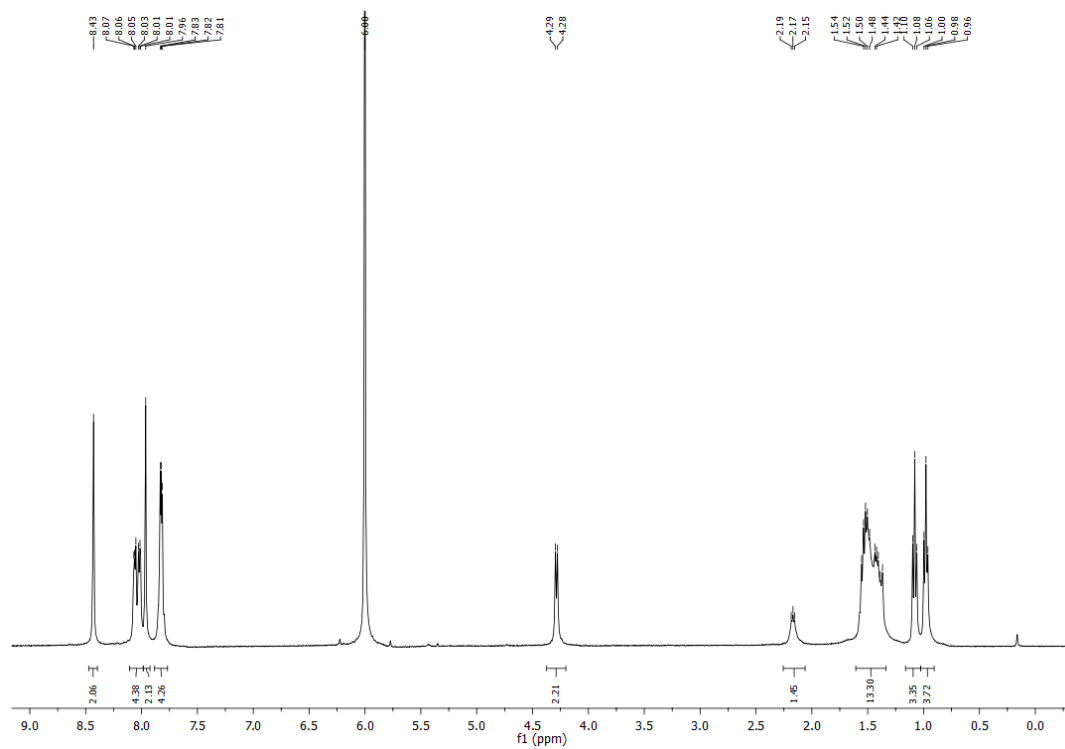


Fig. S7 <sup>1</sup>H NMR of compound 1a (400 MHz, CDCl<sub>2</sub>CDCl<sub>2</sub>, 125 °C).

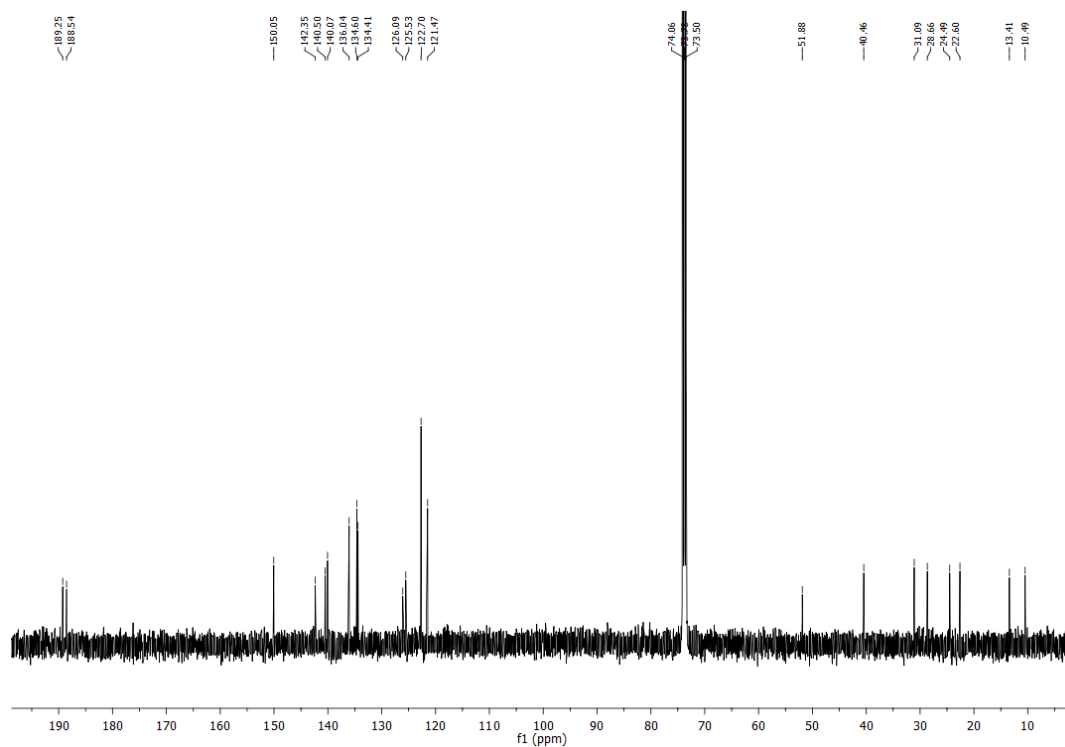
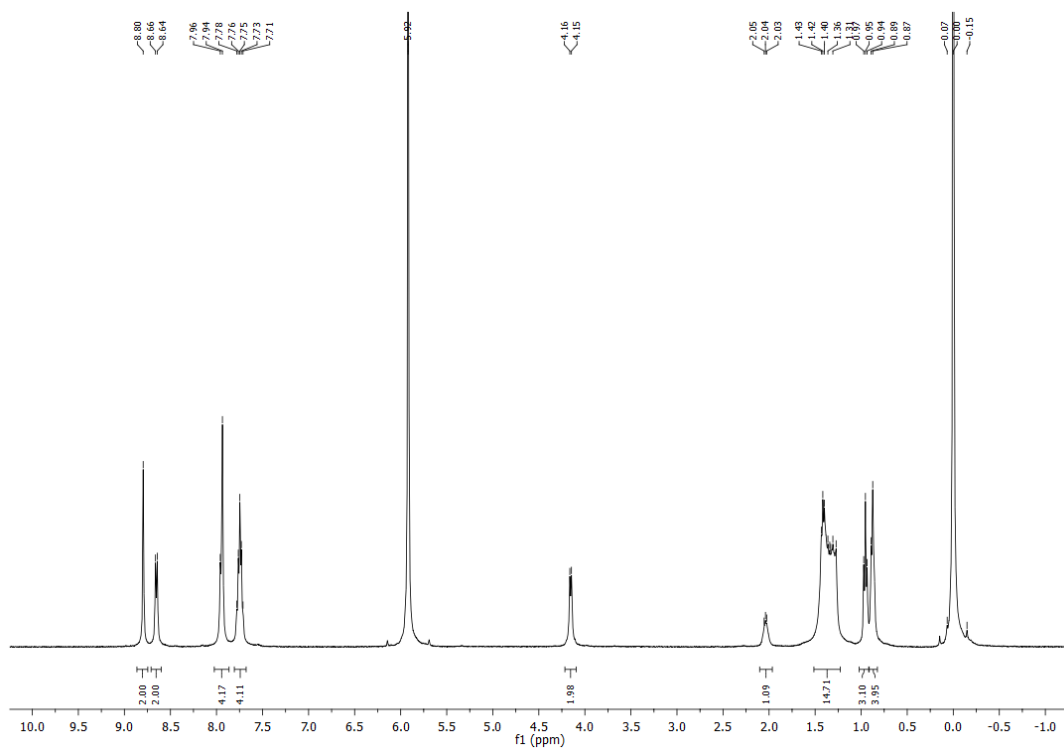
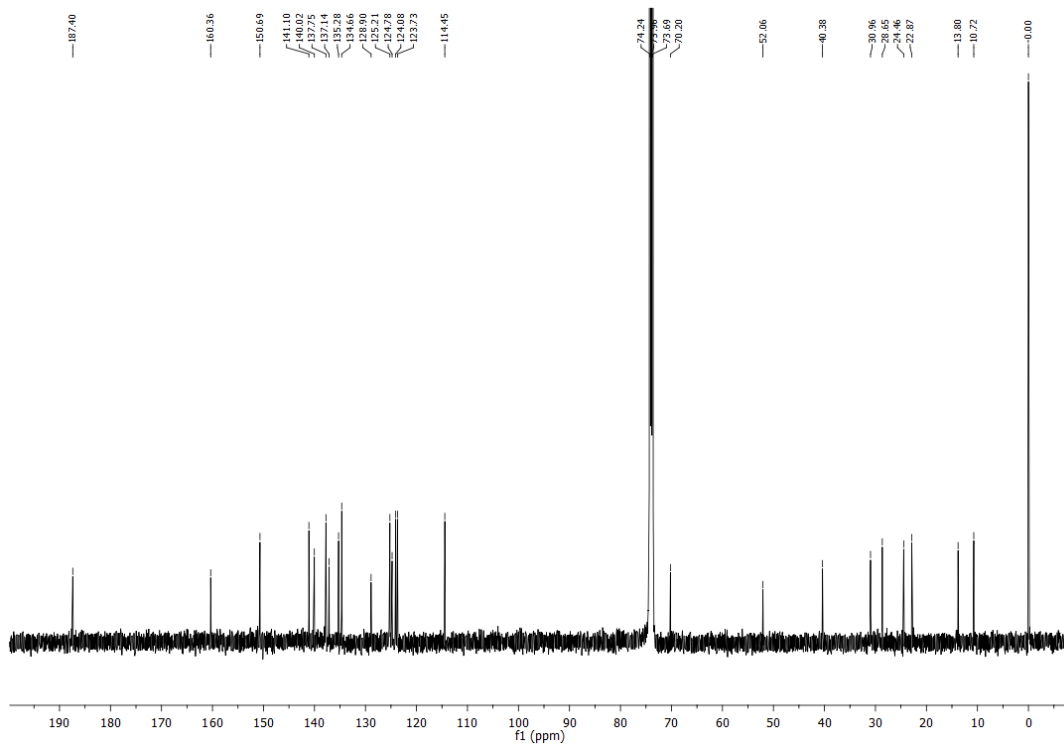


Fig. S8 <sup>13</sup>C NMR of compound 1a (101 MHz, CDCl<sub>2</sub>CDCl<sub>2</sub>, 125 °C).



**Fig. S9**  $^1\text{H}$  NMR of compound **1b** (400 MHz,  $\text{CDCl}_2\text{CDCl}_2$ , 125  $^\circ\text{C}$ ).



**Fig. S10**  $^{13}\text{C}$  NMR of compound **1b** (101 MHz,  $\text{CDCl}_2\text{CDCl}_2$ , 125  $^\circ\text{C}$ ).

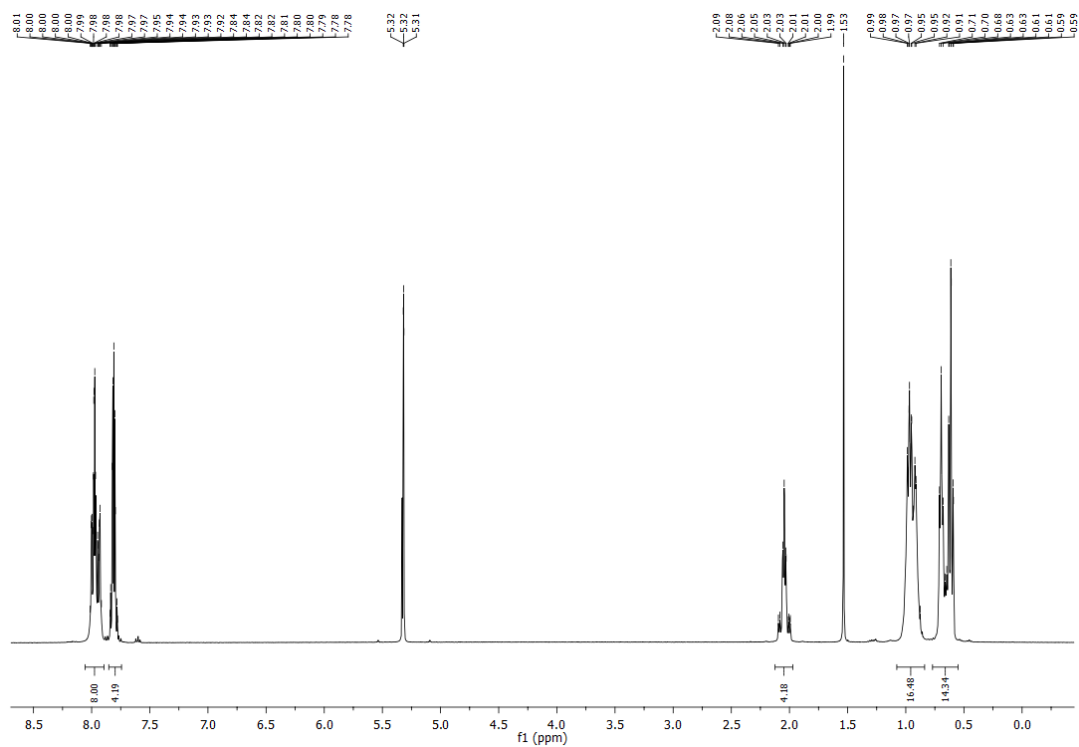


**Fig. S11**  $^1\text{H}$  NMR of compound **2a** (400 MHz,  $\text{CD}_2\text{Cl}_2$ , 25 °C).

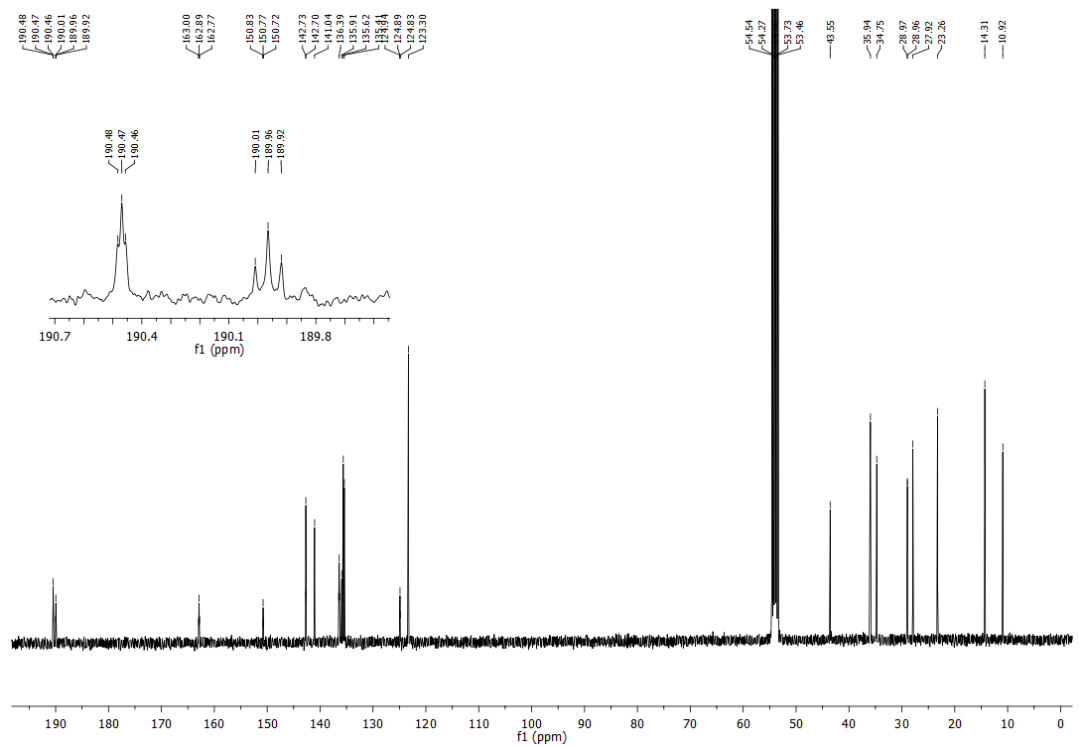


**Fig. S12**  $^{13}\text{C}$  NMR of compound **2a** (101 MHz,  $\text{CD}_2\text{Cl}_2$ , 25 °C).

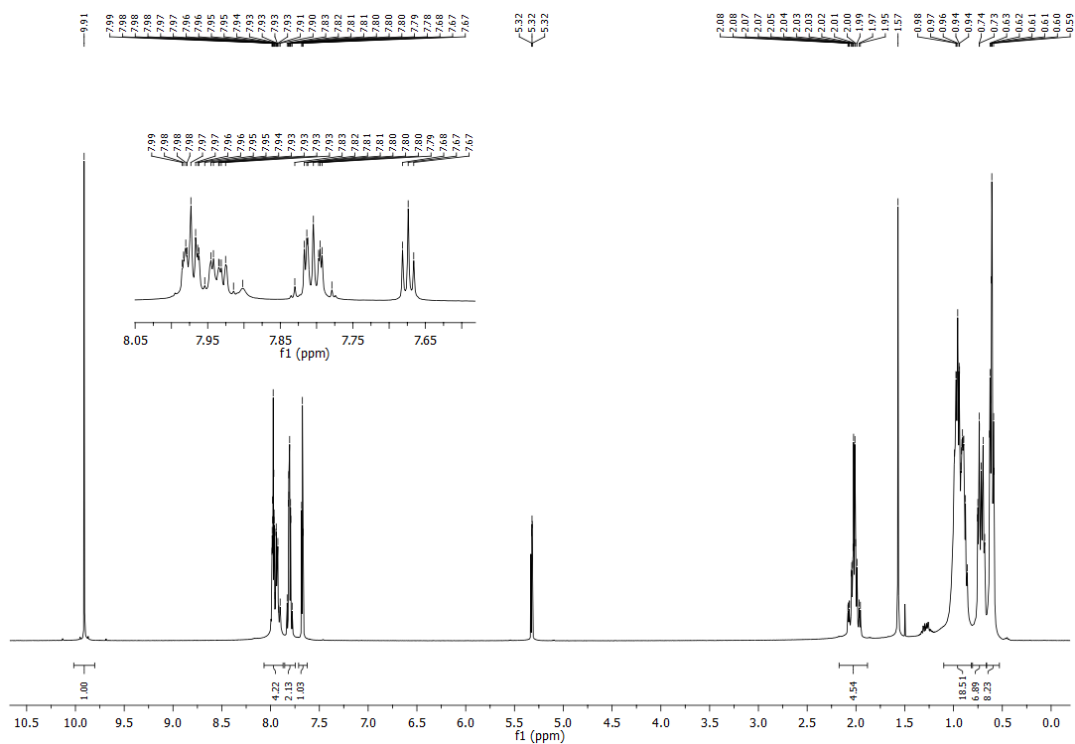


Fig. S13  $^1\text{H}$  NMR of compound  $2a^m$  (400 MHz,  $\text{CD}_2\text{Cl}_2$ , 25  $^\circ\text{C}$ ).

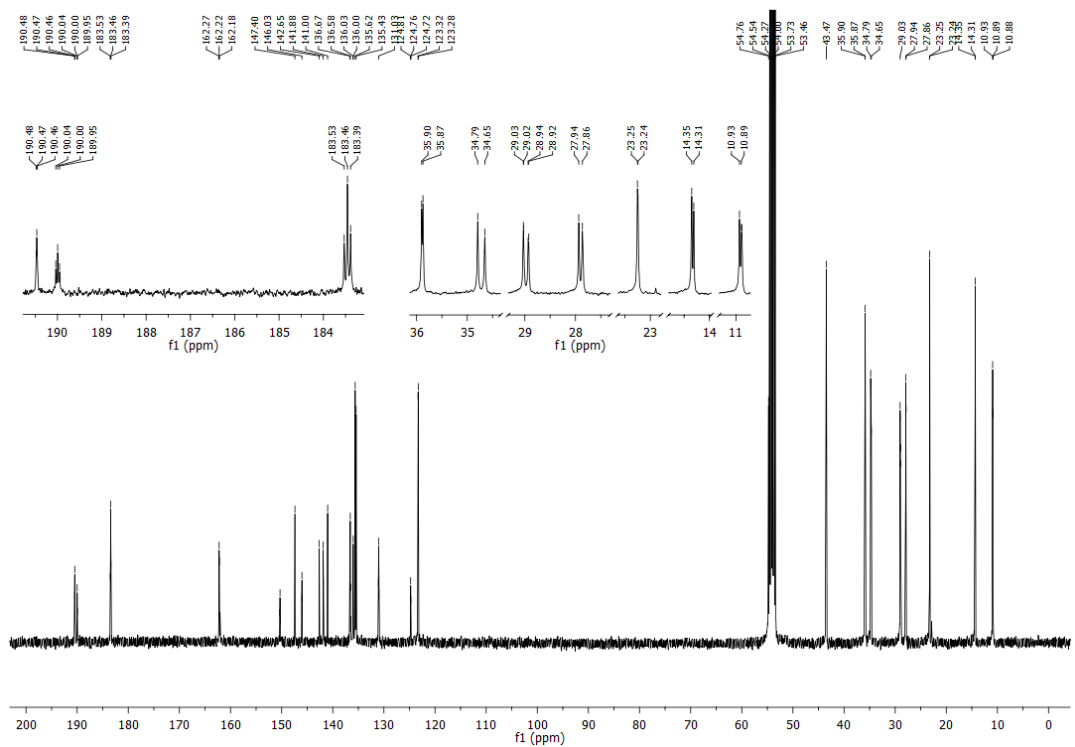
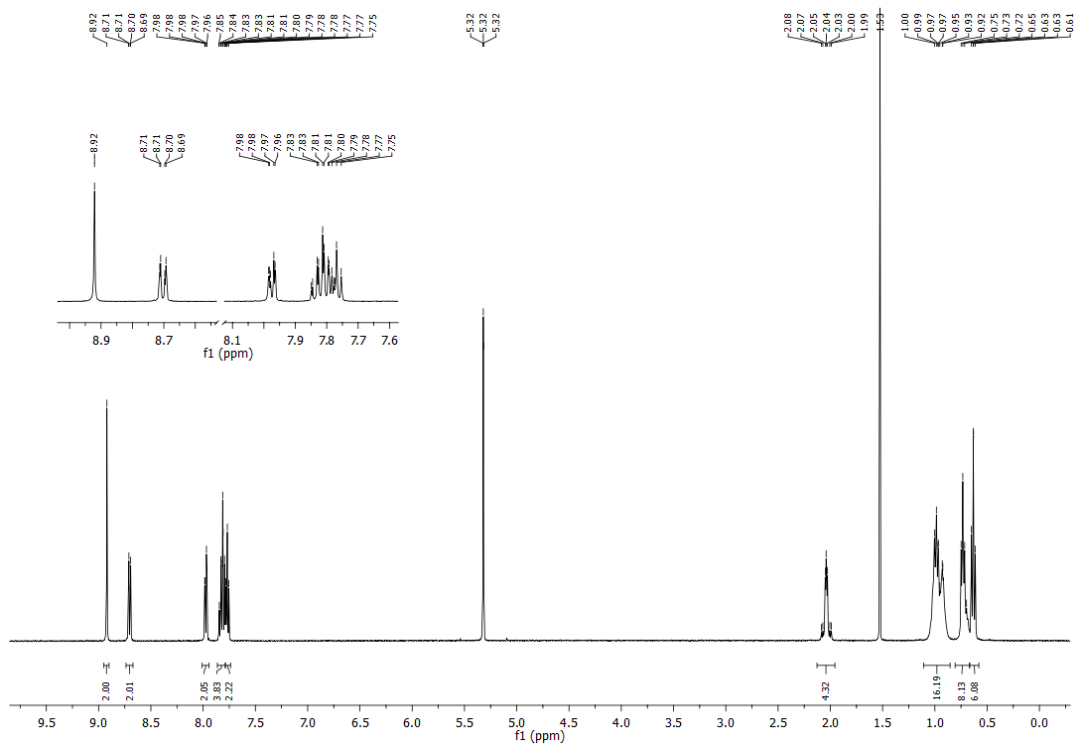
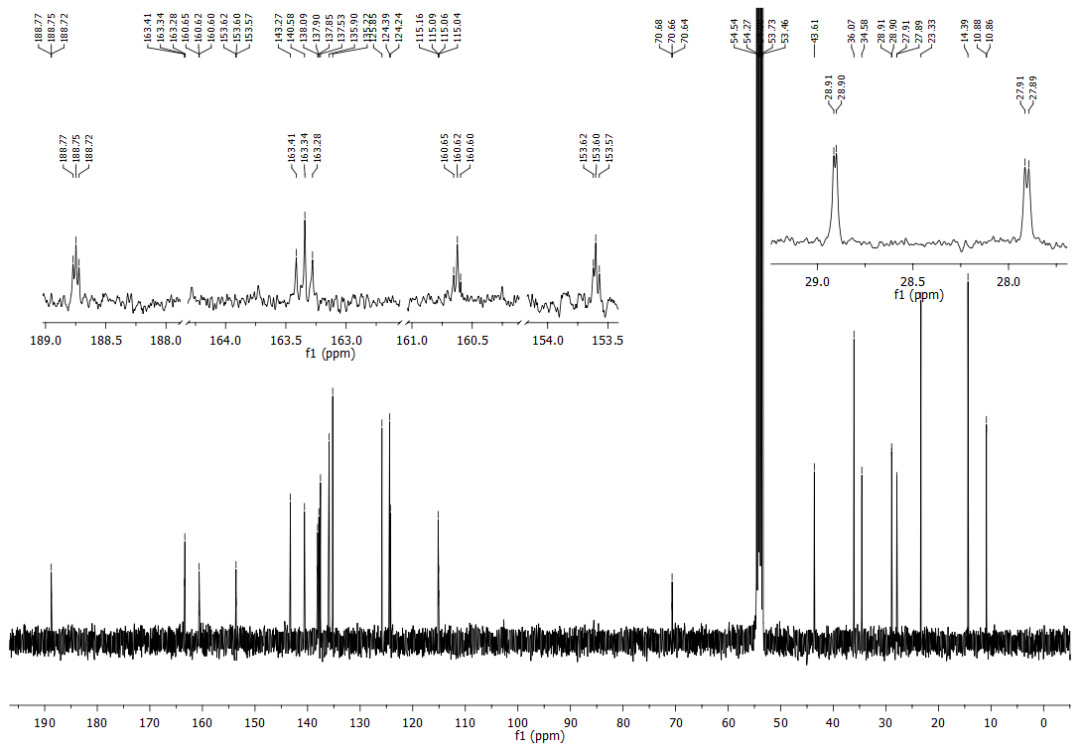


Fig. S14  $^{13}\text{C}$  NMR of compound  $2a^m$  (101 MHz,  $\text{CD}_2\text{Cl}_2$ , 25  $^\circ\text{C}$ ).



**Fig. S15**  $^1\text{H}$  NMR of compound **2b** (400 MHz,  $\text{CD}_2\text{Cl}_2$ , 25 °C).



**Fig. S16**  $^{13}\text{C}$  NMR of compound **2b** (101 MHz,  $\text{CD}_2\text{Cl}_2$ , 25 °C).

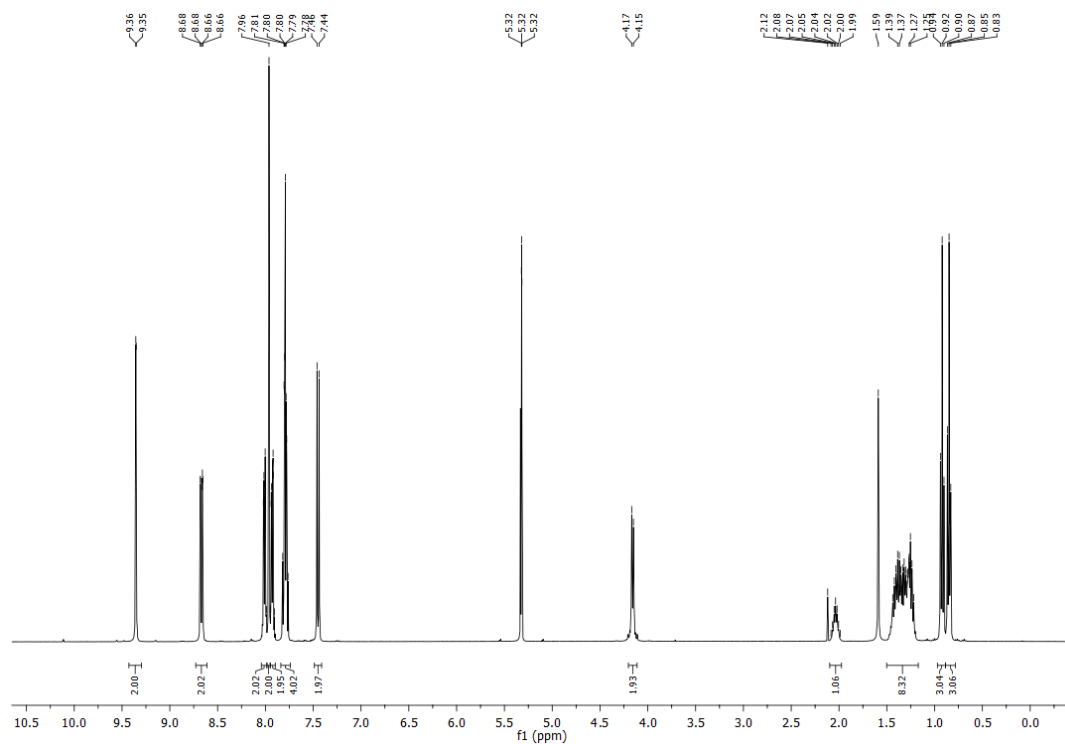


**Fig. S17**  $^1\text{H}$  NMR of compound **3a** (400 MHz,  $\text{CD}_2\text{Cl}_2$ , 25 °C).

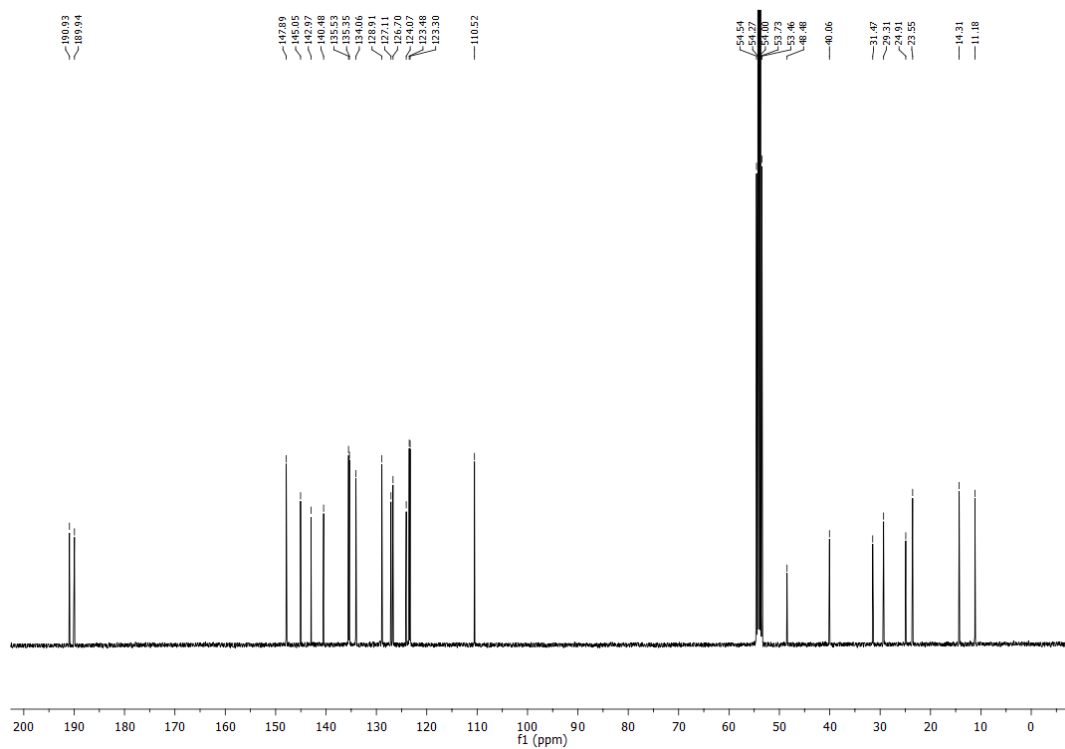


**Fig. S18**  $^{13}\text{C}$  NMR of compound **3a** (101 MHz,  $\text{CD}_2\text{Cl}_2$ , 25 °C).







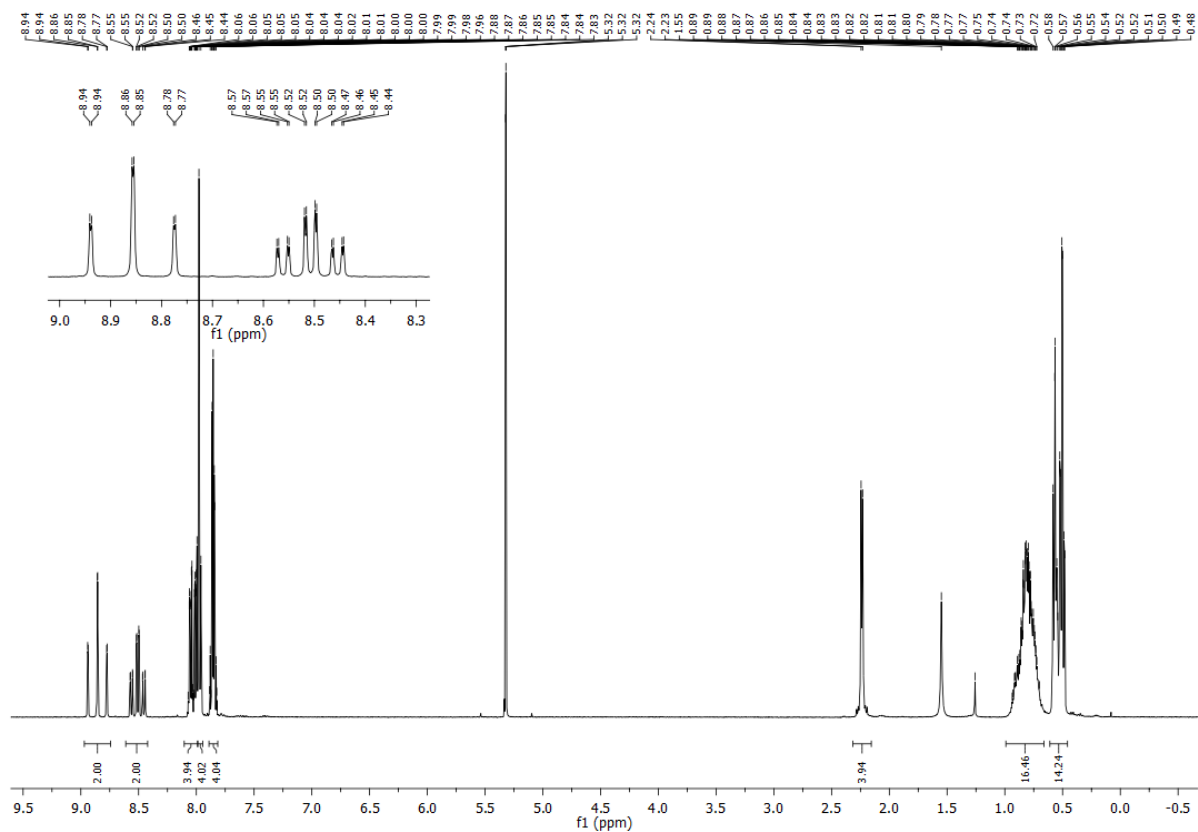


Fig. S25  $^1\text{H}$  NMR of compound **4a** (400 MHz,  $\text{CD}_2\text{Cl}_2$ , 25 °C).

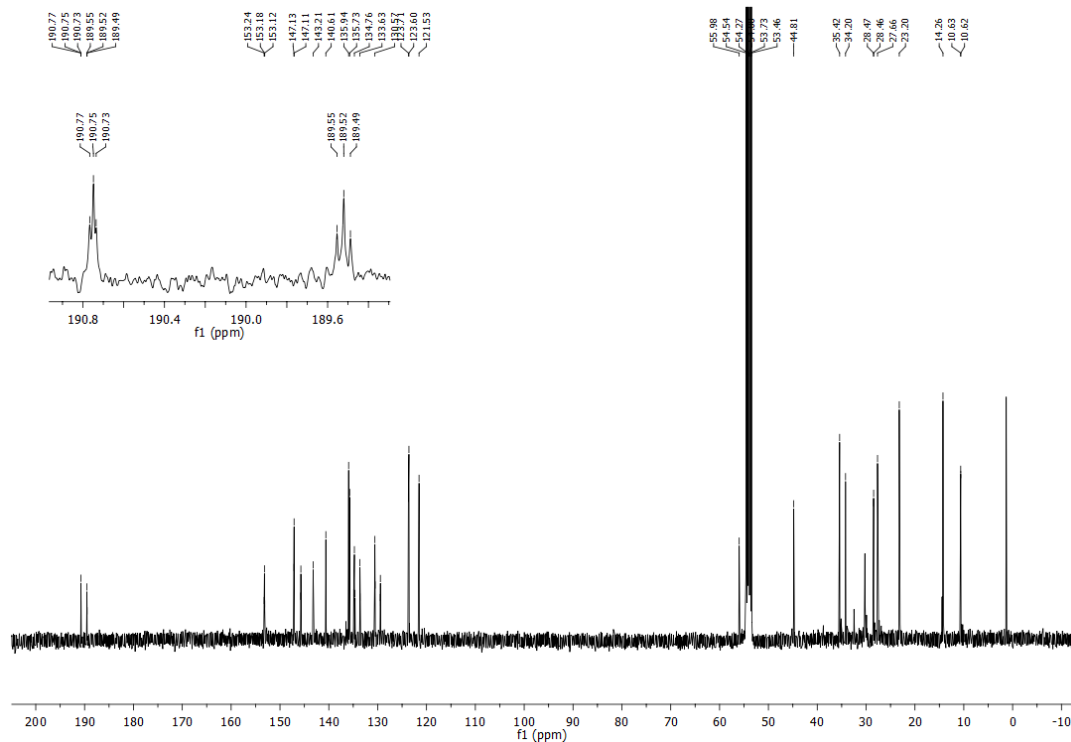


Fig. S26  $^{13}\text{C}$  NMR of compound **4a** (101 MHz,  $\text{CD}_2\text{Cl}_2$ , 25 °C).



## 10. MS spectra

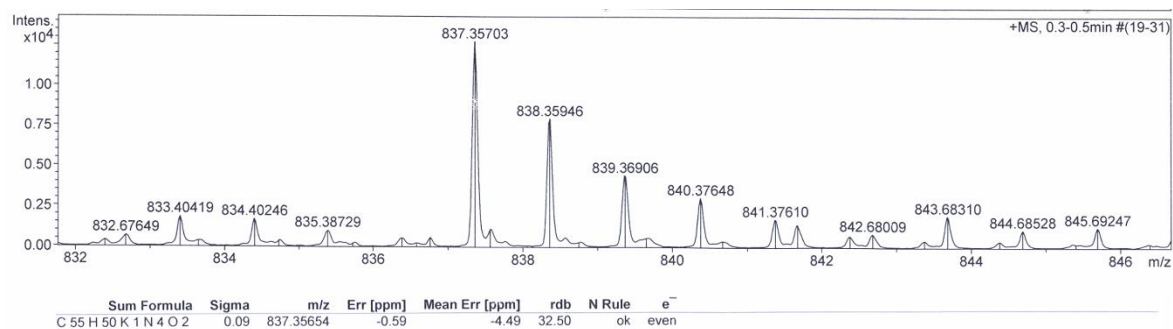


Fig. S29 ESI MS spectrum of compound **4b**.

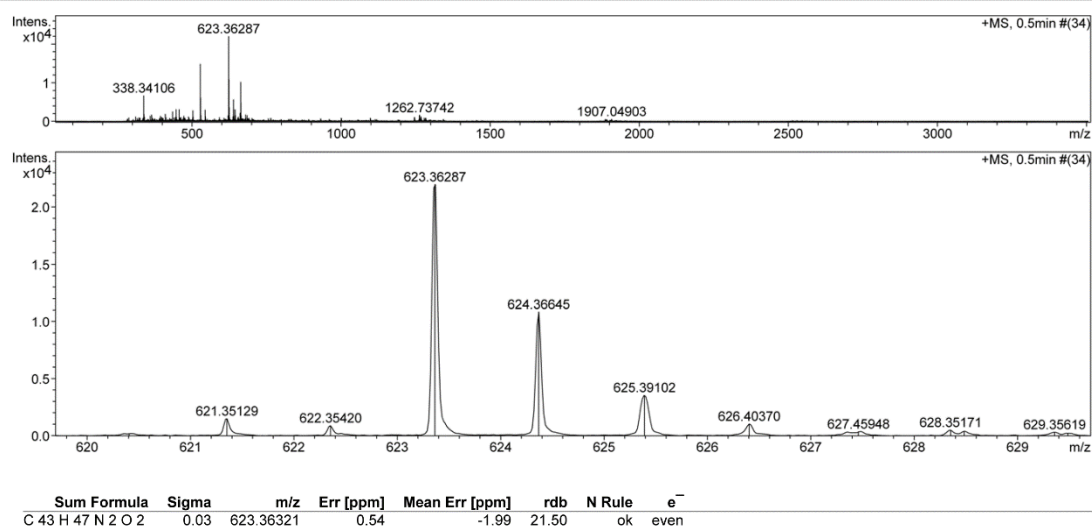


Fig. S30 ESI MS spectrum of compound **4b<sup>m</sup>**.